

P.P. RAJEEV<sup>1,\*</sup>  
S. SENGUPTA<sup>2</sup>  
A. DAS<sup>2</sup>  
P. TANEJA<sup>1</sup>  
P. AYYUB<sup>1</sup>  
P.K. KAW<sup>2</sup>  
G.R. KUMAR<sup>1,✉</sup>

# Laser absorption in short-lived metal and nanoplasmas

<sup>1</sup>Tata Institute of Fundamental Research, 1, Homi Bhabha Road, Mumbai 400005, India

<sup>2</sup>Institute for Plasma Research, Bhat, Gandhi Nagar, India

Received: 3 December 2004 /

Revised version: 23 March 2005

Published online: 31 May 2005 • © Springer-Verlag 2005

**ABSTRACT** We have studied the absorption of 100 fs, 806 nm laser pulses in both bulk and nanoparticulate forms of copper as a function of the electric field intensity as well as polarization. In particular, we have investigated the changes in absorption over a wide range of intensity (over four orders of magnitude) which enables us to study the transition of a metal to plasma. We have found that, even in its nanoparticulate form, the onset of plasma formation occurs in copper when the incident light field intensity is about  $10^{14}$  W cm<sup>-2</sup>. The values of the dielectric permittivities, calculated using the Drude theory, deviate from the room temperature values beyond the onset of plasma formation.

PACS 78.67.Bf; 61.46.+w; 52.38-r; 52.38.Dx

## 1 Introduction

Recent advances in laser technology have provided tools to explore the behaviour of matter under extreme conditions. The advent of intense, ultrashort (subpicosecond) lasers based on the chirped pulse amplification (CPA) technique [1] has created a new realm of light-matter interaction research at high intensities (for an excellent review, see [2]). The ultrafast regime of interaction is fundamentally distinct from the nanosecond regime – there are striking differences between the plasma formed by a nanosecond pulse and that created by a subpicosecond pulse. In the latter, the high field is switched on so rapidly that the detachment of the first electron is completed at substantially higher field strengths, resulting in a rapid electron acceleration to keV energies [3]. Apart from the fundamental physics interest, the study of intense, ultrashort light-matter interaction has opened up a plethora of applications. For example, matter irradiated with intense, ultrashort laser pulses may be regarded as an exceptionally bright, yet tabletop source of X-ray pulses that can be used for time-resolved studies, high-resolution imaging and precision laser machining [2]. Energetic and highly charged ion emission is

also observed from these plasmas, which might be extremely useful for applications ranging from ion implantation to tumor treatment. Further, these plasmas are found to house the largest magnetic fields yet available, with exciting futuristic applications. It is, therefore, crucial to have a clear understanding of the intensity threshold at which plasma is formed on various materials and the mechanism of laser absorption in these plasmas, which could provide us with thumb-rules to optimize and control the laser-plasma coupling.

Several attempts have been made to understand the mechanisms of femtosecond laser absorption in plasmas. Most of them involve studies of the emissions of X-rays and harmonics from the plasma. We know that in the intensity regime of interest, there are two major absorption mechanisms through which laser light is coupled to the plasma, viz. inverse bremsstrahlung (IB) and resonance absorption (RA) [4]. However, a study of the emissions from the plasma to understand the absorption mechanism is at best an indirect procedure. Reflectivity measurements, on the other hand, yield direct information about the plasma formation threshold and the absorption processes within the plasma [5]. Here, we investigate the absorption of infrared (806 nm) light in copper in its bulk as well as nanoparticulate forms. We measure the reflectivity of a single beam of laser pulses: at sufficiently high intensities, the leading edge of the pulse forms plasma on the metal and the remaining part gets reflected from it. Though similar studies over a wide intensity range have been reported on several metals [5, 6], their validity for novel structures, such as nanocrystalline metals does not appear to have been investigated. Such a study has immediate relevance as such nanostructures have been recently shown to significantly enhance the hot electron generation in plasmas [7].

Optically polished copper surfaces were used to ensure specular reflection. Plasma with an appreciable scale length ( $L \geq \lambda$ , where  $\lambda$  is the wavelength of incident radiation) scatters light due to the non-uniformity of the critical layer and instabilities developing in plasma. We have observed in pre-pulse studies that the scattering component becomes relevant as the plasma scale length increases. However, in single pulse studies with femtosecond pulses, the reflection is essentially specular as the plasma has a sharp density gradient. These conditions apply even in the case of nanocrystalline copper surface. Since the nanoparticles are coated very uniformly over an optically polished Cu surface, and since the average particle size ( $\approx 15$  nm) is much smaller than the wavelength of

✉ Fax: +91-22-2280-4610, E-mail: grk@tifr.res.in

\*Present Address: Steacie Institute for Molecular Sciences, National Research Council of Canada, Ottawa, ON, K1A 0R6, E-mail: rajeev.pattathil@nrc.gc.ca

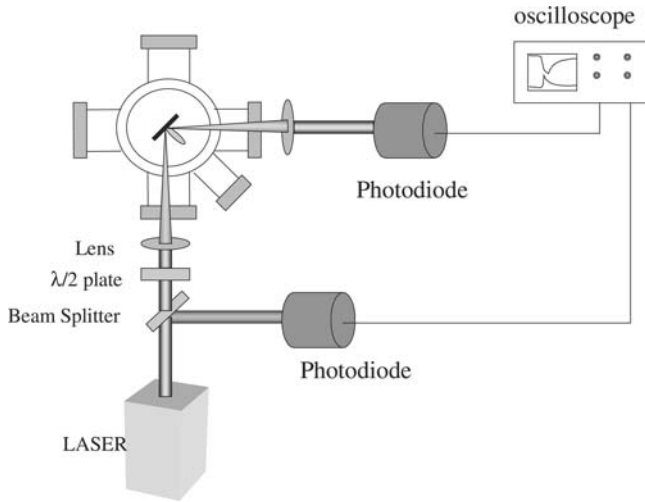


FIGURE 1 Schematic diagram of the experimental set-up

the incident light, the reflection from them is also essentially specular. We observe that even in its nanoparticulate form, Cu has a plasma formation threshold similar to its bulk state. Dielectric functions of bulk copper and copper nanoparticles derived from the reflectivity curves also indicate this point.

## 2 Experimental

The laser used for the experiments described here is a custom-designed chirped pulse amplification [1] Ti: Sapphire system. It is capable of producing 55 mJ pulses of 100 fs duration, at 10 Hz, with a spectral bandwidth of about 20 nm, centred at 806 nm. These parameters amount to a maximum peak power of 0.5 TW per pulse. However, only a maximum of about 10 mJ is used in the present series of experiments, yielding a light intensity of about  $3 \times 10^{16} \text{ W cm}^{-2}$  at a focal spot of 30  $\mu\text{m}$  diameter. Figure 1 schematically depicts the experimental set-up. A 30-cm focal length plano-convex lens focused the linearly polarized laser pulses on to solid targets mounted inside the vacuum chamber, leading to plasma formation at the focal point. A thin half-wave plate introduced in the beam path allowed the beam polarization to be switched between the horizontal (p) and vertical (s) states. The target was constantly rotated and translated to avoid multiple hits at the same spot by the laser pulses. The reflected light was collected by a lens and detected by a photodiode or an integrating sphere. Fluctuations and variations in the input intensity were monitored by a beam-splitter of known transmission ratio and a detector. With properly calibrated detectors, it is possible to obtain absolute reflectivity values for known transmission characteristics of the chamber windows.

In order to obtain the dielectric response function of copper at the operating wavelength, the linear absorption spectrum was measured Fig. 2 using a Shimadzu UV-2100 UV-visible spectrophotometer. The specular reflection was recorded with the incident angle being set to  $8^\circ$ , while the light scattered in  $2\pi$  directions was recorded at normal incidence, using an integrating sphere. In the latter case, the specular part of the reflected light goes back to the source and the scattered light is collected by the integrating sphere internally coated with

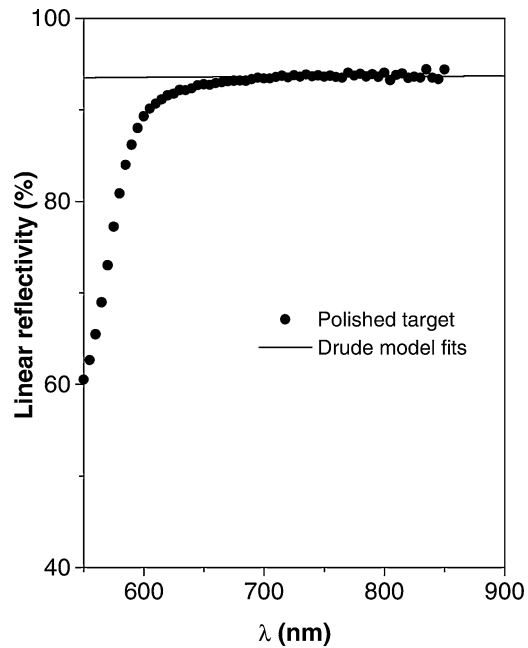


FIGURE 2 Linear Reflectivity spectrum of polished (bulk) copper at normal incidence

white powder (MgO), such that all the scattered light reaches the photomultiplier tube after multiple reflection. The scattering was observed to be negligible. This is further evidenced by the fact that the measured specular reflectivity, without any corrections, is quite close to the value reported in literature [8].

## 3 Results and discussions

### 3.1 Bulk Copper

A study of the reflectivity spectrum of bulk Cu Fig. 2 clearly indicates that interband absorption occurs only below 650 nm. Thus, the Drude free-electron gas model can be used to describe the reflectivity at longer wavelengths. In Drude theory [9], the dielectric function of a metal depends only on the frequency of light, as the collisional frequency is assumed to be independent of wavelength. These assumptions are valid only in the long wavelength regime, where the energies are lower than the inter-band transition energy. We have performed Drude model fits in the higher wavelength regime (see Fig. 2) to determine the collisional frequency by choosing an optimal value that gives the best fit throughout the relevant wavelength range. This value of collision frequency is then used to obtain the real and imaginary parts of the dielectric functions ( $\epsilon = \epsilon' + i\epsilon''$ ) from the Drude equations. At 800 nm, which is quite far from the inter-band transition regime, the fit yields a permittivity value  $\epsilon(800 \text{ nm}) = -27 + i2.5$ , which is quite close to the values reported in literature [8].

To explore the absorption of infrared light (806 nm) in bulk Cu at higher light field intensities, we measured the specularly reflected laser light from a Cu target housed in a vacuum chamber as a function of incident laser intensity. Figure 3 shows the reflectivity curves for p- and s-polarized light as a

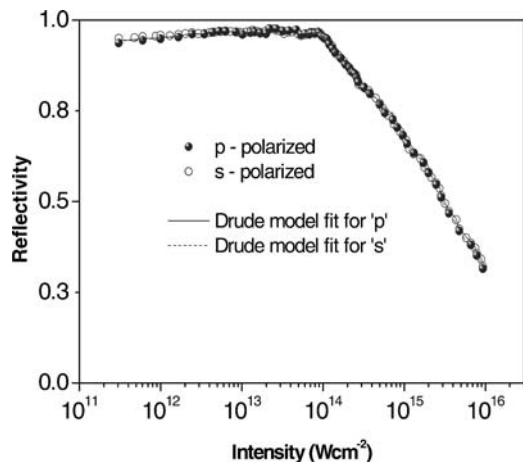


**FIGURE 3** Variation of the reflectivity (at 806 nm) of bulk copper as a function of incident intensity for  $s$ - and  $p$ -polarizations at  $10^\circ$  incidence

function of incident laser intensity ( $10^{11}$ – $10^{16}$   $\text{W cm}^{-2}$ ) at  $10^\circ$  incidence. Clearly, the reflectivity does not vary much with polarization in the linear regime, especially for small angles of incidence.

The most interesting feature in the data is the continuous drop of reflectivity above  $10^{14}$   $\text{W cm}^{-2}$ . This is an indication of a considerable degree of plasma formation at these intensity levels and the resulting absorption of light. It is possible to obtain a reasonable estimate of the intensity required for plasma formation from simple calculations. The plasma formation threshold for copper is calculated to be a few times  $10^{13}$   $\text{W cm}^{-2}$  in recent literature [10, 11]. Our observed value is quite close to these predictions. Hence, reflectivity studies can clearly provide an idea of the plasma formation threshold in a material. At intensities below the plasma formation threshold, the incident laser pulse is reflected from the metal surface, and, consequently, the reflectivity is high. As the peak intensity is increased, the pulse starts to form a plasma at the focal point. Plasma formation occurs at the leading edge if the peak intensity is high compared to the plasma formation threshold ( $10^{14}$   $\text{W cm}^{-2}$  in our case) and the remaining part of the pulse then gets reflected from the plasma. Since the plasma is an absorbing medium, the net reflectivity drops once the peak intensity crosses the plasma formation threshold. After the plasma formation, the polarization dependence of absorption increases as compared to the same in a metal. The  $p$ -polarized light fields are known to couple better to the plasma at larger angles due to certain extra absorption channels that open up as a result of electrostatic waves set-up along the density gradient. This is caused by the component of electric field along the density gradient, normal to the target surface [4]. However, at small angles of incidence, the component of electric field along the normal to the target (along the plasma density gradient) is too small to be effective even for  $p$ -polarization. Thus, there is no significant difference in the reflectivities of  $s$ - and  $p$ -polarized light even after the plasma formation, as observed in Fig. 3.

It is important to examine how the metal dielectric functions responsible for the reflectivity behave at these extreme light intensities. Intensity dependent values of the real and imaginary parts of dielectric functions were obtained from

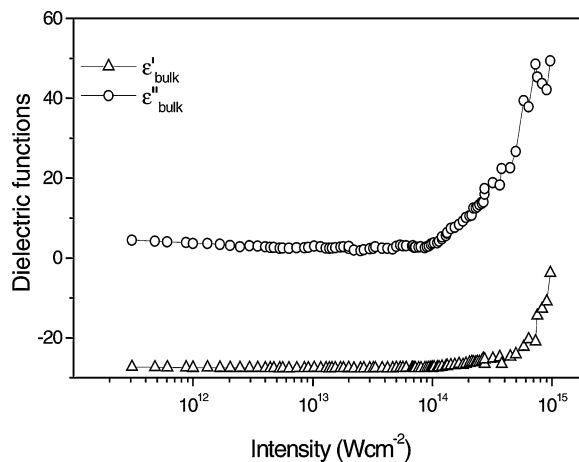


**FIGURE 4** Real and imaginary parts of the dielectric functions of bulk copper as a function of incident light intensity

the intensity dependent reflectivity data for  $s$ - and  $p$ -polarized light. For this purpose, we used a MATLAB code similar to the one earlier used to obtain Drude model fits, but with the following differences: (a) Instead of adjusting the collision frequency, the real and imaginary parts of  $\epsilon$  were adjusted such that the calculated reflectivities match the observed values for the  $s$ - and  $p$ -polarized light, (b) This procedure was not performed for the data as a whole, but separately for each intensity point—solving two equations (for the reflectivities) with two variables ( $\epsilon'$  and  $\epsilon''$ ) at each intensity, and (c) Instead of a minimization routine, we used a routine for solving non-linear equations. The solution is also based on the concept of minimizing errors. Fresnel formulae were used for obtaining reflectivities [5].

Figure 4 depicts the variation of the dielectric functions of copper as a function of light intensity. Even at intensities as large as  $10^{14}$   $\text{W cm}^{-2}$ , the values of  $\epsilon'$  and  $\epsilon''$  do not show any change, which is expected since the reflectivity also remains constant up to this intensity regime. As the reflectivity starts dropping at intensities greater than  $10^{14}$   $\text{W cm}^{-2}$ , the dielectric functions, too, deviate from the linear values. Note that the imaginary part of the dielectric function, which is indicative of the collisional absorption in the metal/plasma changes faster than the real part that depends mainly on the free-electron content in the medium. The collisional absorption increases drastically as the ionization starts and the electrons are freed. The value of the plasma formation threshold obtained in our experiment is quite close to that suggested by Zhang et al., based on a simple ionization model [10].

The onset of plasma formation can also be investigated by creating conditions wherein polarization sensitive absorption mechanisms accompany the plasma formation. For example, an obliquely incident,  $p$ -polarized light field is preferentially absorbed in a plasma because of the excitation and damping of electrostatic Langmuir waves set-up in the plasma by the component of light field along the density gradient [4]. The field tunneling in from the reflection point, and hence the oscillation amplitude, undergoes a resonance at the critical density layer in the plasma, resulting in a strong absorption of the  $p$ -polarized light. This resonance absorption [4] is considered to be the major source of hot electrons in laser-produced plasmas

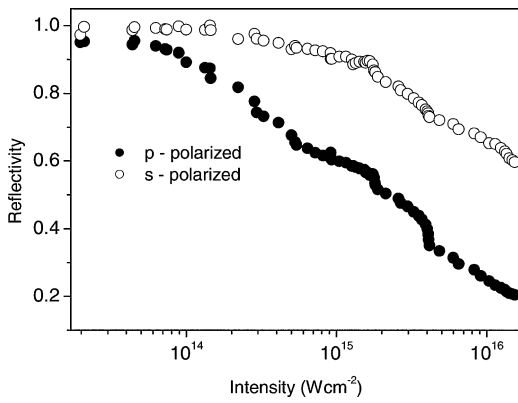


**FIGURE 5** Variation of the reflectivity (at 806 nm) of bulk copper as a function of incident light intensity for *s*- and *p*-polarizations at 50° incidence

in the intensity range of investigation. However, *s*-polarized light fields lack any component along the density gradient and do not excite any electrostatic waves in the plasma. The difference between the reflectivities of *p*- and *s*-polarized lights should therefore increase from its Fresnel values once the plasma is formed.

Figure 5 shows the intensity dependence of the self-reflectivity of *s*- and *p*-polarized laser fields incident at 50°, soon after the plasma formation. As seen earlier, plasma begins to form when the peak intensity is around  $10^{14} \text{ W cm}^{-2}$ . The difference between *s* and *p* reflectivity is the same as the Fresnel value obtained for Cu, before the plasma formation. However, as is evident from the figure, *p*-polarized light is absorbed to a greater extent than its *s*-polarized counterpart, as soon as the plasma is formed. Non-collisional absorption mechanisms (largely resonance absorption under our experimental conditions) dominate the interaction of *p*-polarized light and result in a greater coupling. The increase in the absorption of *s*-polarized light is due mainly to the increase in the collisional frequency on plasma formation. Depolarization in the non-ideal focusing geometry and the consequent extra absorption could also play a role in the excess absorption of *s*-polarized fields and even the hot-electron generation by them.

### 3.2 Nanocrystalline Copper

We now examine the changes in the absorption in presence of sub-wavelength surface structures such as nanoparticles that are expected to significantly affect the laser coupling and subsequent hot electron production [7]. In particular, we investigate the behaviour of copper nanoparticles exposed to intense fields. Slightly ellipsoidal copper nanoparticles were deposited by high-pressure dc-magnetron sputtering [12] on copper substrates. The sputtering was carried out in a custom-built chamber using a 200 mm long, axial, planar magnetron source (Atom Tech 320-O). The sputtering target was a copper disc of 50 mm diameter, placed 55 mm away from the substrate. The base pressure was better than  $10^{-6}$  Torr, while sputtering was carried out in the presence of flowing Ar or He, at a pressure between 100 and 200 m Torr. At such relatively high pressures, the sputtered copper atoms

lose much of their kinetic energy in colliding with the gas atoms and arrive at the substrate with little energy left for surface diffusion. Optically polished copper discs were used as substrates (held at  $-50^\circ\text{C}$ ). The nanocrystalline films typically consist of a collection of densely packed nanoparticles. Details of production and characterization of nanocrystalline films are reported elsewhere [13]. The sputter-deposited Cu films are optically flat and their thickness ( $1 \mu\text{m}$ ) is greater than the skin depth of the laser light in use. The coherently diffracting crystallographic domain size ( $d_{\text{XRD}}$ ) is obtained from X-ray diffraction line broadening, using the Scherrer technique [14]. For a film deposited in 180 mTorr Ar at a sputtering power of 200 W, we obtain  $d_{\text{XRD}} = 15 \text{ nm}$ . The aspect ratio is obtained from a comparison of  $d_{\text{XRD}}$  calculated from (1 1 1) and (2 0 0) diffraction lines. The ellipsoidal particles were found to have an aspect ratio of 1.5.

As in the case of the optically polished target, the linear reflectivity spectrum was used to estimate the linear dielectric functions of the nanocrystalline sample. The reflectivity is about 60% in the linear regime as compared to over 90% for bulk copper (Fig. 2) for wavelengths greater than 650 nm [7]. The reflectivity spectrum for nano-Cu was fitted with the Drude formula and the dielectric functions obtained as before. For nanoparticles with an average diameter of 15 nm, the fit yields permittivity  $\epsilon' + i\epsilon''$  to be  $-3.8 + i10.5$  at 800 nm. However, the reflecting layer is composed not only of nanoparticles, but also of voids between them. Thus, the reflecting medium should be regarded as a composite of nanoparticles and air, such that effective medium theories need to be used to find out the net dielectric constant of the nanoparticles. Using the generalized Bruggeman effective medium approximation [15], the permittivity of the nano-Cu system was obtained as  $-27 + i44.4$ , as compared to  $-27 + i2.5$ , the permittivity of bulk copper. Extensive studies have been carried out on the variation of the dielectric constant of metals with particle size [16]. The real part of the dielectric constant is shown to be unaffected in most systems, unless the particle size is extremely small. The imaginary part increases due to the limited electron mean-free path in the nanoparticles [17]. The values of the imaginary part obtained by us above are, however, much larger than theoretically predicted values by Kreibitz et al. [17], and it is quite likely that the discrepancy is due to the factors such as dipole interactions between neighbouring particles that are excluded in the theoretical modelling.

We now examine the polarization and intensity dependence of absorption in the nanoparticles. As in the case of polished targets, a single laser beam was reflected from an optically polished Cu target coated with Cu nanoparticles. The input intensity of the laser beam was varied over a large range ( $10^{12}$ – $10^{16} \text{ W cm}^{-2}$ ) and the change in reflectivity observed as a function of the incident intensity and polarization. Figure 6a shows the self-reflectivity measurements in nanoparticles as a function of intensity, for the two different polarizations. The interesting feature in the low intensity region is the strong polarization dependence of reflection even at a comparatively low incidence angle of  $22.5^\circ$ . In contrast, a comparable difference in absorption of the *s* and *p*-polarized light fields in polished targets requires the angle of incidence to be greater than  $50^\circ$ , as evident from Fig. 5. The enhanced sensitivity of nanocrystalline targets towards light polarization is the result



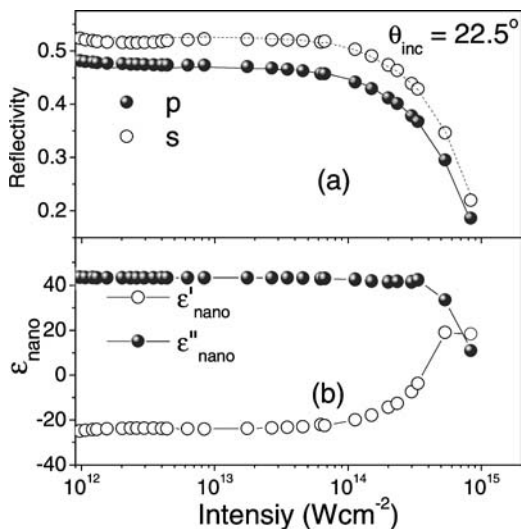


FIGURE 6 Variation of **a** reflectivity and **b** dielectric functions of ellipsoidal copper nanoparticles at 806 nm with incident light intensity

of the surface wave absorption existing in structured surfaces. Surface waves are allowed excitation modes along the interface of a metal and a dielectric medium and their quanta are surface plasmons [18]. In normal metallic reflection in vacuum, light is not coupled to this mode because an extra component of wave-vector is required to connect the “vacuum light-line” (the dispersion curve of light in vacuum) to the surface plasmon dispersion curve. This extra wave-vector may be provided by structures such as gratings or nanocrystalline surfaces that allow light to be coupled to this mode and eventually damped. The additional absorption and subsequent local electric field enhancement near such nanostructures originate from surface plasmon excitations, which are highly polarization sensitive. From the dispersion relation of surface plasmons, we find that only the  $p$ -polarized light fields (which supply electric field components normal to the target) induce surface plasmon modes. This is the reason for the polarisation dependence of reflectivity being quite evident even at small incidence angles, where even the small component of electric field along the surface normal is efficiently absorbed.

Figure 6 depicts the variation of reflectivity as well as its polarization dependence as the intensity of the incident light field is increased. As in the polished targets, the reflectivity suddenly drops at intensity levels above  $10^{14} \text{ W cm}^{-2}$ , as a result of a substantial plasma formation. The interesting point to note here is that the enhanced polarization sensitivity exists even after the plasma is just formed. This, however, diminishes at higher intensities, where the curves appear to merge. This could be because of the possible deformation of the nanostructure due to the inhomogeneous formation and subsequent expansion of plasma triggered by the inhomogeneous distribution of local fields around the nanostructure. The strong deviation of both the real and imaginary parts of dielectric function, from the metal-values, upon plasma formation could also alter the polarization dependence. It is, nevertheless, important to note that the inherent property of nanoparticles—a strongly polarization dependent absorption—exists even at intensities just after plasma formation. Here, the nanoparticles

behave as nanoplasmas—they are “nanoparticles” with just different dielectric functions.

A Matlab program similar to the one described earlier was used to determine the variation of the dielectric functions of the nanoparticles with intensity. The reflectivity values were back-calculated to verify that they fit the original data. The back-calculated reflectivity curve is plotted using solid lines in Fig. 6a. Figure 6b shows the variation of the dielectric functions with input laser intensity derived from Fig. 6a. The deviation of both the reflectivity as well as the dielectric functions from room temperature values occurs only above  $10^{14} \text{ W cm}^{-2}$ . So, for all practical purposes,  $10^{14} \text{ W cm}^{-2}$  may be considered as a minimum value of the plasma formation threshold both in the case of bulk copper and copper nanoparticles.

#### 4 Conclusion

In conclusion, we have studied the reflection of laser light from optically polished as well as nanoparticulate copper over a wide range of light intensities so as to obtain a better understanding of the absorption pathways both before and after plasma formation. The sudden drop in reflectivity as a function of the incident intensity directly indicates the plasma formation threshold both in polished and nanocrystalline copper targets. The difference in the absorption of the  $s$  and  $p$ -polarized fields also indicates the formation of plasma at the focal point. Using the reflectivity data, we derived the dielectric functions of bulk as well as nanocrystalline copper across the plasma formation threshold. Nanoparticles show an enhanced sensitivity to the polarization state of the light field due to the effect of the highly polarization selective surface plasmon excitation. This property prevails even after a weak plasma is formed on the nanostructures, but is eventually diminished with a strong plasma formation.

#### REFERENCES

- 1 D. Strickland, G. Mourou, *Opt. Commun.* **56**, 219 (1985)
- 2 P. Gibbon, E. Förster, *Plasma Phys. Control. Fusion* **38**, 769 (1996)
- 3 T. Brabec, F. Krausz, *Rev. Mod. Phys.* **70**, 545 (2000)
- 4 W.L. Krueer, *The Physics of Laser Plasma Interactions* (Addison-Wesley, 1988)
- 5 M.K. Grimes, A.R. Rundquist, Y.S. Lee, M.C. Downer, *Phys. Rev. Lett.* **82**, 4010 (1999)
- 6 H.M. Milchberg, R.R. Freeman, S.C. Davey, R.M. More, *Phys. Rev. Lett.* **61**, 2364 (1988)
- 7 P.P. Rajeev, P. Taneja, P. Ayyub, A.S. Sandhu, G.R. Kumar, *Phys. Rev. Lett.* **90**, 115002 (2003)
- 8 P.B. Johnson, R.W. Christy, *Phys. Rev. B* **6**, 4370 (1972)
- 9 N.W. Ashcroft, N.D. Mermin, D. Mermin, *Solid State Physics* (International Thomson Publishing, 1976)
- 10 Y. Zhang, J. Zhang, S.-H. Pan, Y.-X. Nie, *Opt. Commun.* **126**, 85 (1996)
- 11 D. von der Linde, H. Schüller, *J. Opt. Soc. Am. B* **13**, 216 (1996)
- 12 P. Ayyub, R. Chandra, P. Taneja, A.K. Sharma, R. Pinto, *Appl. Phys. A* **73**, 67 (2001)
- 13 P. Taneja, PhD Thesis, Tata Institute of Fundamental Research (2002)
- 14 B. Warren, *X-Ray Diffraction* (Addison-Wesley, Reading, 1969)
- 15 C.G. Granqvist, O. Hunderi, *Phys. Rev. B* **16**, 3513 (1977)
- 16 L. Genzel, T.P. Martin, U. Kreibig, *Z. Phys. B* **21**, 339 (1975)
- 17 U. Kreibig, C.V. Fragstein, *Z. Phys.* **224**, 307 (1969)
- 18 H. Raether, *Surface Plasmons on Smooth and Rough Surfaces and on Gratings* (Springer Berlin Heidelberg New York, 1988)